Mullaney JC, Zaleski DP, Tew DP, Walker NR, Legon AC.

Geometry of an Isolated Dimer of Imidazole Characterised by Broadband Rotational Spectroscopy and Ab Initio Calculations.

***ChemPhysChem* (2016)**

DOI: http://dx.doi.org/10.1002/cphc.201501179

A EUROPEAN JOURNAL

CHEMPHYSCHEM

OF CHEMICAL PHYSICS AND PHYSICAL CHEMISTRY

Accepted Article

Title: Geometry of an Isolated Dimer of Imidazole Characterised by Broadband Rotational Spectroscopy and Ab Initio Calculations

Authors: John C Mullaney; Daniel P Zaleski; David P Tew; Nicholas R Walker; Anthony C Legon

To be cited as: ChemPhysChem 10.1002/cphc.201501179

Link to VoR: http://dx.doi.org/10.1002/cphc.201501179

A Journal of

ChemPubSoc Europe

www.chemphyschem.org

WILEY-VCH

Chem. Phys. Chem.

Geometry of an Isolated Dimer of Imidazole Characterised by Rotational Spectroscopy and Ab Initio Calculations

John C. Mullaney,[†] Daniel P. Zaleski,[†§] David P. Tew,[‡] Nicholas R. Walker[†*] and Anthony C. Legon[‡*]

† School of Chemistry, Bedson Building, Newcastle University, Newcastle upon Tyne, Tyne and Wear, NE1 7RU, U.K.

‡School of Chemistry, University of Bristol, Bristol, BS8 1TS, U.K.

§ [Current address: Argonne National Laboratory, Chemical Sciences & Engineering, 9700 S. Cass Ave., Bldg. 200, Lemont, IL 60439, U.S.A.]

*Corresponding authors email: nick.walker@newcastle.ac.uk, a.c.legon@bristol.ac.uk

KEYWORDS: imidazole, rotational spectroscopy, microwave spectroscopy.

ABSTRACT

An isolated, gas-phase dimer of imidazole has been generated through laser vaporization of a solid rod containing a 1:1 mixture of imidazole and copper in the presence of an argon buffer gas undergoing supersonic expansion. The complex is characterized through broadband rotational spectroscopy and is shown to have a twisted, hydrogen-bonded geometry. Calculations at the CCSD(T)(F12*)/cc-pVDZ-F12 level confirm this to be the lowest energy conformer of the imidazole dimer. The distance between the respective centres of mass of the imidazole monomer sub-units is determined to be 5.2751(1) Å while the "twist" angle (describing rotation of one monomer with respect to the other about a line connecting the centres of mass of the respective monomers), γ, is determined to be 87.9(4)°. Four out of six intermolecular parameters in the model geometry are precisely determined from the experimental rotational constants and are consistent with results calculated *ab initio*.

1. Introduction

Imidazole ($C_3H_4N_2$) comprises a five-membered, aromatic ring that contains both pyrrolic and pyridinic nitrogen atoms. The coordinative properties of imidazole result from the donor/acceptor properties of its two nitrogen atoms and its amphoteric character.[1] The frequencies of intermolecular N–H···N stretching modes have been measured for various species embedded within a helium nanodroplet including an imidazole dimer[2], a trimer[3] and complexes where each of these units is respectively attached to H_2O. N-heterocyclic molecules are also a central component of natural and artificial photochemical systems.[4] Recent research has extensively explored the photochemistry and fragmentation dynamics of imidazole and other N-heterocyclics.[5] This work reports the broadband rotational spectrum of a neutral imidazole dimer generated and isolated in the gas phase. The spectrum is analysed to experimentally characterise the geometry of the interaction between two imidazole monomers independent of matrix or solvent effects for the first time.

The $(C_3H_4N_2)_2$ complex is generated by vaporization of imidazole from a solid target rod by the focused pulse from a Nd:YAG laser (532 nm, 10 mJ pulse^{-1}) in the presence of argon introduced from a pulsed-gas injection nozzle. The target rod is initially prepared by compressing powdered material using a benchtop press. Experiments that led to the first observation of rotational transitions of $(C_3H_4N_2)_2$ used a rod prepared from copper and imidazole powders (in a 1:1 molar ratio). Replacement of this rod with a second prepared from imidazole and activated carbon powders brings no measurable change in the intensities of observed transitions of $(C_3H_4N_2)_2$. However, transitions of $(C_3H_4N_2)_2$ are significantly weaker if the rod is prepared from imidazole only (with no included carbon or copper). Immediately subsequent to the laser pulse, the gas mixture undergoes supersonic expansion and species within the jet are rotationally and vibrationally cooled. The intensities of transitions assigned to $(C_3H_4N_2)_2$ imply a rotational temperature on the order of 2 K for this species. The broadband rotational spectrometer used for this work detects transitions across a 12 GHz bandwidth in a single measurement and has been described in detail previously.[6]

2. Results and Discussion

Intense transitions observed within the spectrum (Figure 1) assign to the imidazole monomer previously studied by Christen *et al*.[7] Other observed transitions can be readily assigned to CH_3CN,[8] CH_3CH_2CN,[9] CH_2CHCN,[10] HCCCN,[11] NH_2CH_2CN,[12] HC_5N,[13] HC_7N,[14] and CH_3C_3N[15] which have all previously been studied by microwave spectroscopy. Evidently, a fraction of imidazole molecules undergoes fragmentation and further reactions subsequent to vaporization from the solid target rod. The sequence of chemical reactions that yields the various products listed above is not explored by this work but similar behavior has been observed by broadband rotational spectroscopy before.[16] It can also be noted that the photochemistry and fragmentation dynamics of imidazole and other N-heterocyclic molecules have been explored in detail elsewhere, mode-specific product formation being an interesting result of UV photolysis of imidazole.[17] Other transitions in the observed spectrum do not assign to any species for which a microwave spectrum has previously been reported. This work will demonstrate that these assign to a $(C_3H_4N_2)_2$ complex in which two imidazole monomer sub-units interact via an intermolecular hydrogen bond.

Full geometry optimisation of the imidazole dimer at the CCSD(T)(F12*)/cc-pVDZ-F12 level[18] of theory is prohibitively expensive owing to the present lack of analytic gradients. To approximate this level of accuracy, the geometry of the monomer and dimer were first optimised at the MP2 level of theory to identify which geometric parameters change significantly upon complexation. The only parameter that changes significantly on formation of the dimer is the N–H bond length involved in the hydrogen bond. A CCSD(T)(F12*)/cc-pVDZ-F12 geometry optimisation was then performed for the dimer in the space of six inter-molecular coordinates and the N–H bond length, keeping the remaining structural parameters fixed at values optimised for the monomers. The results of both our *ab initio* calculations and those performed previously by Choi *et al*.[2] are consistent with the twisted, H-bonded geometry (shown in Figure 2) being the minimum energy conformation for the dimer. The pyrrolic N–H group of one imidazole monomer is calculated to form a hydrogen bond with the pyridinic nitrogen on the second. The resulting imidazole dimer is axially

chiral. Coordinates and optimized values of structural parameters are provided for both the isolated imidazole monomer and the described dimer in Supplementary Data Table 1. For the purposes of this work, the monomer acting as H-bond acceptor within the intermolecular bond will hereafter be referred to as "monomer 1" while the H-bond donor will be labelled as "monomer 2". At the CC2/aug-cc-pVTZ level of theory, the $(C_3H_4N_2)_2$ complex is calculated to possess a dipole moment of 9.1 D in the twisted, H-bonded geometry. The calculated rotational constants informed a search of the broadband spectrum, with the result shown in Figure 1. Discounting transitions for which molecular carriers had already been reported in previous works (as summarized above), structured patterns of transitions are found at intervals of ~900 MHz, broadly consistent with expectations for a dimer in the geometry presented in Figure 2. There is excellent agreement between the rotational constants implied by the interval between $J' \rightarrow J''$ transitions and those predicted for the twisted, hydrogen-bonded geometry predicted *ab initio*. The observation of *a*-type transitions in the spectrum is also consistent with the calculated orientation of the dipole moment which is close to parallel with the *a* inertial axis. No *b*- or *c*- type transitions were identified which is consistent with their lower calculated values and current sensitivity limits.

Measurement of the spectra of isotopically-substituted species was achieved through the use of isotopically-enriched samples of imidazole. $C_3D_4N_2$ was obtained from a commercial supplier (CDN Isotopes) allowing measurement of the spectrum of the $(C_3D_4N_2)_2$ isotopologue. $C_3H_3N_2D$ was synthesized by boiling CH_3OD in the presence of $C_3H_4N_2$, driving the H/D isotopic exchange selectively at the hydrogen atom attached to the pyrrolic nitrogen. The spectra of $(C_3H_3N_2D)_2$ and $(C_3H_4N_2)(C_3H_3N_2D)$ were then recorded through measurements using samples respectively prepared from (i) a 1:1 mixture of copper and $C_3H_3N_2D$ and (ii) a 2:1:1 mixture of copper, $C_3H_3N_2D$ and $C_3H_4N_2$. Two geometries are possible for the $(C_3H_4N_2)(C_3H_3N_2D)$ isotopomer, distinct in respect of whether the single deuterium atom is substituted into the pyrrolic N–H bond that forms the intermolecular hydrogen bond. The spectrum of only one isotopologue of $(C_3H_4N_2)(C_3H_3N_2D)$ was observed, shifted from the spectrum of $(C_3H_4N_2)_2$ by only a very small amount, consistent with placement of the D atom very close to the centre of mass in the complex. This suggests assignment of the spectrum to the isotopologue wherein the D atom is positioned between the two monomers and

participates in the intermolecular bond in the twisted, H-bonded geometry. The alternative isotopologue of $(C_3H_4N_2)(C_3H_3N_2D)$ was not apparent in the spectrum. This effect, whereby the relative stabilities of different isotopologues (having the same empirical formula) apparently depends on the position of the substituted atom(s), has been noted previously[19]. Spectra were measured and assigned for four isotopologues of the imidazole dimer in total.

It will be shown that the spectrum of $(C_3H_4N_2)_2$ is consistent with an asymmetric rotor which is very close to the prolate symmetric rotor limit. In such cases, there is a centrifugal distortion-induced splitting of K_{-1} = n doublets (in addition to the usual asymmetry splitting) which becomes detectable. This effect increases rapidly with increasing J and has been shown[20,21] to be most significant for transitions having K_a = 2. During the present work, a preliminary fit of the data was performed using Western's PGOPHER[22] and Watson's S reduction[23] (I^r representation) to give A_0, B_0, C_0 and the quartic centrifugal distortion constants Δ_J, Δ_{JK} and d_1. It thus became apparent that many transitions having K_a =2 are split by an interval greater than can be explained by the magnitude of the rotational constants alone. This additional splitting scales with $(J+1)^3$ as expected for an effect caused by centrifugal distortion and is great enough to resolve only for transitions where $J' > 12$. The S/N of affected transitions is not great enough to quantify this effect for the $(C_3H_3N_2D)_2$ isotopologue. The splitting is fitted to $4D_3(J+1)^3$ to determine mean values of D_3 for each of the $(C_3H_4N_2)_2$, $(C_3H_4N_2)(C_3H_3N_2D)$ and $(C_3D_4N_2)_2$ isotopologues. Correction factors calculated from these are applied to the observed frequencies of K_a=2 transitions yielding corrected transition frequencies that are included in each final fit of measured transitions to a model Hamiltonian (Table 1). Details of the calculations to determine the mean values of D_3 are provided in Supplementary Data Tables 2-4.

Values of B_0, C_0, D_J and D_{JK} are determined very precisely for all isotopologues and do not depend significantly on the reduction applied to the Hamiltonian. Lower precision is associated with the evaluated A_0, d_1 and D_3 while d_2 cannot be determined. Various conformations of the imidazole dimer that have been calculated by Choi *et al.*[2] to lie at higher energy than the twisted, H-bonded dimer have $B_0 - C_0$ between 40 and 50 MHz. This is significantly greater than the <2 MHz difference between B_0 and C_0 identified for all of the various isotopologues described herein. The isotopic shifts

and recorded transition frequencies are therefore consistent only with assignment to a dimer of imidazole in the geometry shown in Figure 2. Although the imidazole monomer contains two ^{14}N nuclei, each having spin (I=1), hyperfine splittings were not observed in the spectra. All ^{14}N quadrupole coupling constants of the imidazole monomer are of the order of 3 MHz.[7] Hyperfine splittings decrease with increasing J and only $J' \rightarrow J''$ transitions having $J' > 8$ are observed by the present experiments. Splittings introduced by nuclear quadrupole coupling with the framework angular momentum are evidently insufficiently large to resolve. Complete details of the spectroscopic fits to determine the various spectroscopic parameters are included as Supplementary Data Table 5.

2.1 Molecular Geometry

The experimentally-measured rotational constants allow quantitative determination of parameters in the model geometry. Data are available only for the ground vibrational state so r_0 parameters are determined. The geometry of each imidazole monomer is assumed unchanged from the r_0 geometry of the imidazole monomer,[7] except that a small correction is made to the length of the N–H bond in the pyrrolic group that participates in the intermolecular bond. This parameter is calculated to extend by 0.016 Å in the r_e geometry and the same extension is assumed to occur within the r_0 geometry for the complex. Six intermolecular coordinates are used to define the geometry of the dimer with reference to the inertial axis systems of the respective imidazole monomers. The first three parameters describe the relative positions of these monomers and are R_{cm}, the distance between the centres of mass (com) of the imidazole monomer sub-units; θ and φ, respectively polar and azimuth angles used to locate the position of the com of monomer 2 with respect to the com of monomer 1. The final three intermolecular coordinates are used to define the orientation of monomer 2 with respect to monomer 1. α and β are angles defined between the c and b axes (respectively) of monomer 2 and the line connecting the com of the two monomers. γ is the dihedral angle between (i) the plane containing the c axis of monomer 1 and the line connecting the coms of the two monomers and (ii) the plane containing the c axis of monomer 2 and the line connecting the coms of the two monomers. With the aid of Figure 3, α, β and γ may be respectively visualized as the tilting of monomer 2 toward

or away from monomer 1 (α), turning of monomer 2 in the plane of itself (β) and twisting of monomer 2 about the line connecting the coms of the two monomers (γ). With reference to the vectors shown in Figure 3, the various angles are explicitly defined as follows where $|\boldsymbol{v}_n|$ are magnitude vectors and $\boldsymbol{b}_n$ are normalized vectors.

$$|\boldsymbol{v}_3||\boldsymbol{v}_2|\cos(\alpha) = \boldsymbol{v}_3 \cdot \boldsymbol{v}_2 \quad (1)$$

$$|\boldsymbol{v}_1||\boldsymbol{v}_2|\cos(\beta) = \boldsymbol{v}_1 \cdot \boldsymbol{v}_2 \quad (2)$$

$$|\boldsymbol{v}_2||\boldsymbol{v}_4|\cos(\theta) = \boldsymbol{v}_2 \cdot \boldsymbol{v}_4 \quad (3)$$

$$\phi = \mathrm{atan2}\left(\left[[\boldsymbol{b}_1 \times \boldsymbol{b}_2] \times \boldsymbol{b}_2\right] \cdot [\boldsymbol{b}_2 \times \boldsymbol{b}_3], [\boldsymbol{b}_1 \times \boldsymbol{b}_2] \cdot [\boldsymbol{b}_2 \times \boldsymbol{b}_3]\right) \quad (4)$$

$$\gamma = \mathrm{atan2}\left(\left[[\boldsymbol{b}_4 \times \boldsymbol{b}_1] \times \boldsymbol{b}_1\right] \cdot [\boldsymbol{b}_1 \times \boldsymbol{b}_2], [\boldsymbol{b}_4 \times \boldsymbol{b}_1] \cdot [\boldsymbol{b}_1 \times \boldsymbol{b}_2]\right) \quad (5)$$

The available data do not allow all intermolecular parameters to be fitted[24] from the twelve experimentally-determined rotational constants. Fixing θ and α at their values (both equal to 90°) calculated *ab initio* is reasonable given the evidence presented for the twisted, H-bonded geometry illustrated in Figure 2. The assumption that θ = 90° is equivalent to assuming that the com of monomer 2 lies in the plane of monomer 1. Likewise, C–H groups adjacent to the intermolecular bond on each imidazole monomer are oriented such that any movement away from α = 90° (ie tilting of the plane of one monomer towards or away from the plane of the other) will be strongly hindered. The remaining four intermolecular parameters are fitted to obtain the results shown in Table 2. The values of R_{cm} and γ are very sensitive functions of the evaluated rotational constants and are precisely determined. The φ and β angles are determined though with larger uncertainties. It is satisfying to note the level of agreement between experiment and theory, particularly given that minimal assumptions are involved in the fitting of the molecular geometry. Figure 2 overlays the geometry calculated *ab initio* with that obtained through fitting to the experimental data. Coordinates of atoms determined through fitting to the experimentally-measured rotational constants are provided in Supplementary Data Table 6.

The ∠N–H…N (intermolecular) bond angle implied by the fit of the r_0 geometry to the experimental data is 169.3° while the *ab initio* calculated results imply 179.6° for the same angle. The length of the intermolecular H-bond implied by the fitted geometry is 1.960 Å while that calculated *ab*

initio is 1.947 Å. When fitting the various geometrical parameters listed in Table 2, an r_0 geometry is initially assumed for each imidazole monomer while the *ab initio* calculation yields parameters in the r_e geometry. These slightly varying initial assumptions lead to the differences between the *ab initio* calculated and experimental geometries. The ∠N–H…N (intermolecular) bond angle is particularly sensitive to these. It is thus concluded that an intermolecular hydrogen bond allows the formation of an imidazole dimer which can be generated for gas phase study by a method that combines laser ablation and supersonic expansion. This synthetic method is similar to that used previously in studies of biomolecules, metal halides and mixed metal species[25]. Noting that spectroscopic experiments are generally assisted by conditions that maximize the intensities of measured transitions, it is empirically observed as beneficial to mix imidazole with an inert matrix (copper metal was used during this work) when preparing the solid starting material. The length of the bond and the geometry of the interaction between two isolated imidazole monomers has thus been accurately determined for the first time.

ACKNOWLEDGMENTS

The authors thank the European Research Council for a postdoctoral fellowship awarded to D.P.Z, for a postgraduate studentship to J.C.M., and for project funding (CPFTMW-307000). A.C.L. thanks the University of Bristol for a Senior Research Fellowship, and Newcastle University for a Faculty of SAgE Visiting Professorship. D.P.Z. thanks Newcastle University for the award of a Faculty of SAgE Research Fellowship. D.P.T. thanks the Royal Society for a University Research Fellowship. The authors also thank Dr. Simon Doherty (School of Chemistry, Newcastle University) for preparing the sample of monodeuterated imidazole necessary for these experiments.

Table 1. Spectroscopic constants determined for four isotopologues of $(C_3H_4N_2)_2$.

Spectroscopic constant	$(C_3H_4N_2)_2$	$(C_3H_4N_2)(C_3H_3DN_2)$[a]	$(C_3H_3DN_2)_2$	$(C_3D_4N_2)_2$
A_0 / MHz	4800(25)	4710(50)	4680(53)	3970(16)
B_0 / MHz	457.53869(27)[b]	457.32707(37)	449.86071(31)	424.53190(40)
C_0 / MHz	456.03871(26)	455.84958(38)	448.01603(31)	422.81625(39)
D_{JK} / kHz	8.3740(54)	8.299(15)	7.828(14)	7.311(11)
$[D_J \times 10^2]$ / kHz	6.907(15)	6.773(22)	6.952(25)	5.926(18)
d_1 / Hz	–2.63(22)	–2.96(29)	–3.39(28)	–2.10(28)
N[c]	63	36	39	43
$\sigma_{r.m.s.}$ / kHz[d]	6.4	7.9	6.9	8.0
D_3 / Hz	3.79(28)[e]	4.4(7)	-	0.56(25)

[a] See text for an unambiguous description of the geometry of this isotopologue.
[b] Numbers in parentheses are one standard deviation in units of the last significant figure.
[c] Number of transitions included in the fit.
[d] rms deviation of the fit.
[e] Values of D_3 are fitted separately (see text and Supplementary Data Tables 2-4 for details).

Table 2. Structural parameters in the model geometry of $(C_3H_4N_2)_2$.

	Exp.	CCSD(T)(F12*)/VDZ (r_e)
A_0 / MHz[a]	4800(25)	4864.02
B_0 / MHz	457.53869(27)	454.07
C_0 / MHz	456.03871(26)	453.91
Parameter	Exp. (r_0)	CCSD(T)(F12*)/VDZ (r_e)
R_{CM} / Å	5.2751(1)	5.297
θ / °	[90]	90.0
ϕ / °	106.3(50)	99.9
α / °	[90]	90.0
β / °	122.3(54)	117.4
γ / °	87.9(4)	90.0
r(H…N) / Å	1.960[c]	1.947
∠(NH…N) / °	169.3[c]	179.6

[a] The comparison of computed and experimentally-determined rotational constants is for the $(C_3H_4N_2)_2$ isotopologue. Results for all other isotopologues are in similar agreement.
[b] Numbers in parentheses are one standard deviation in units of the last significant figure.
[c] r(H…N) and ∠(NH…N) are not included in the parameter set fitted to the measured rotational constants. These results are deduced from the values of fitted parameters.

Figure 1

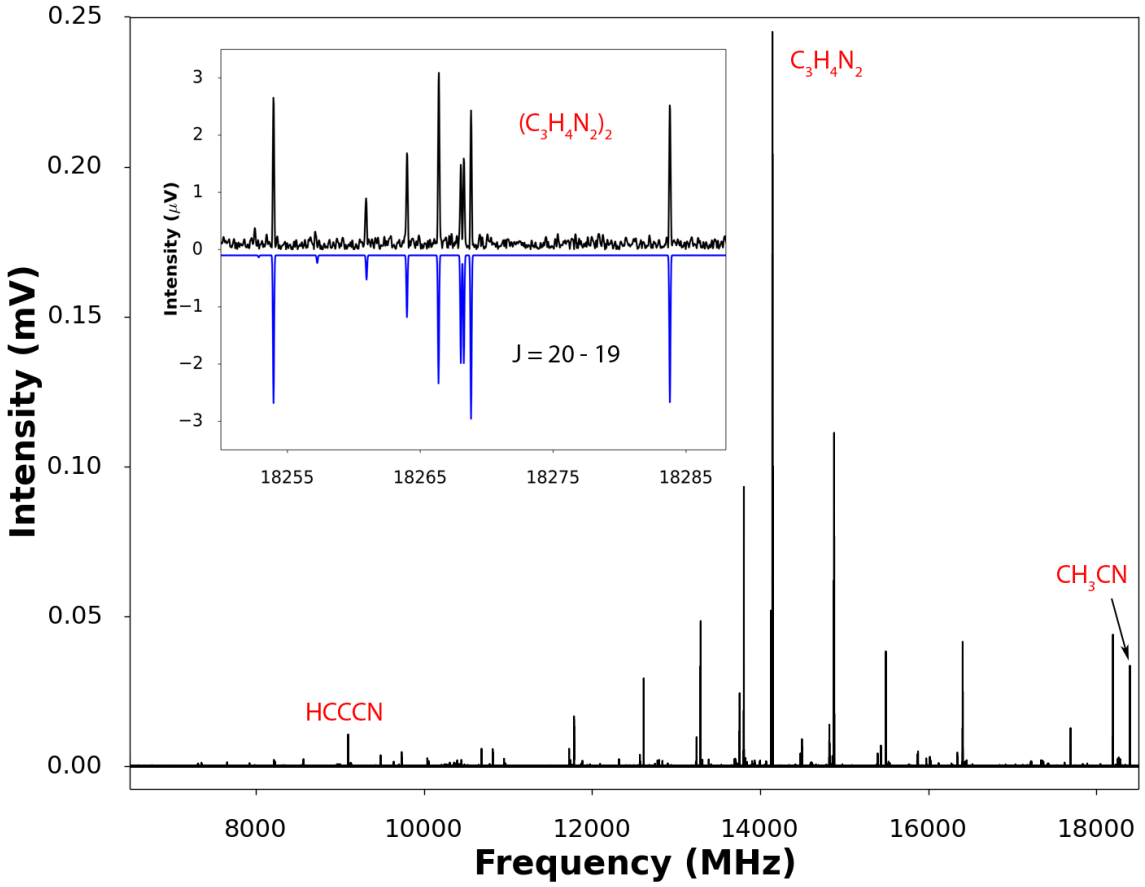

Figure 1

The broadband spectrum obtained when probing an expanding gas sample prepared as described in the text. The displayed spectrum is obtained after co-adding 60k FIDs in the time domain (data collected over a period of 2 hours). The experimental spectrum contains various hydrocarbons in addition to imidazole-containing products. The most intense signals assign to transitions of the imidazole monomer. The inset displays $20_{K'_{-1}\,K'_{+1}} \rightarrow 19_{K''_{-1}\,K''_{+1}}$ transitions in the observed spectrum of

the imidazole dimer above an inverted simulation (blue) that uses the model Hamiltonian and the parameters given in Table 1.

Figure 2

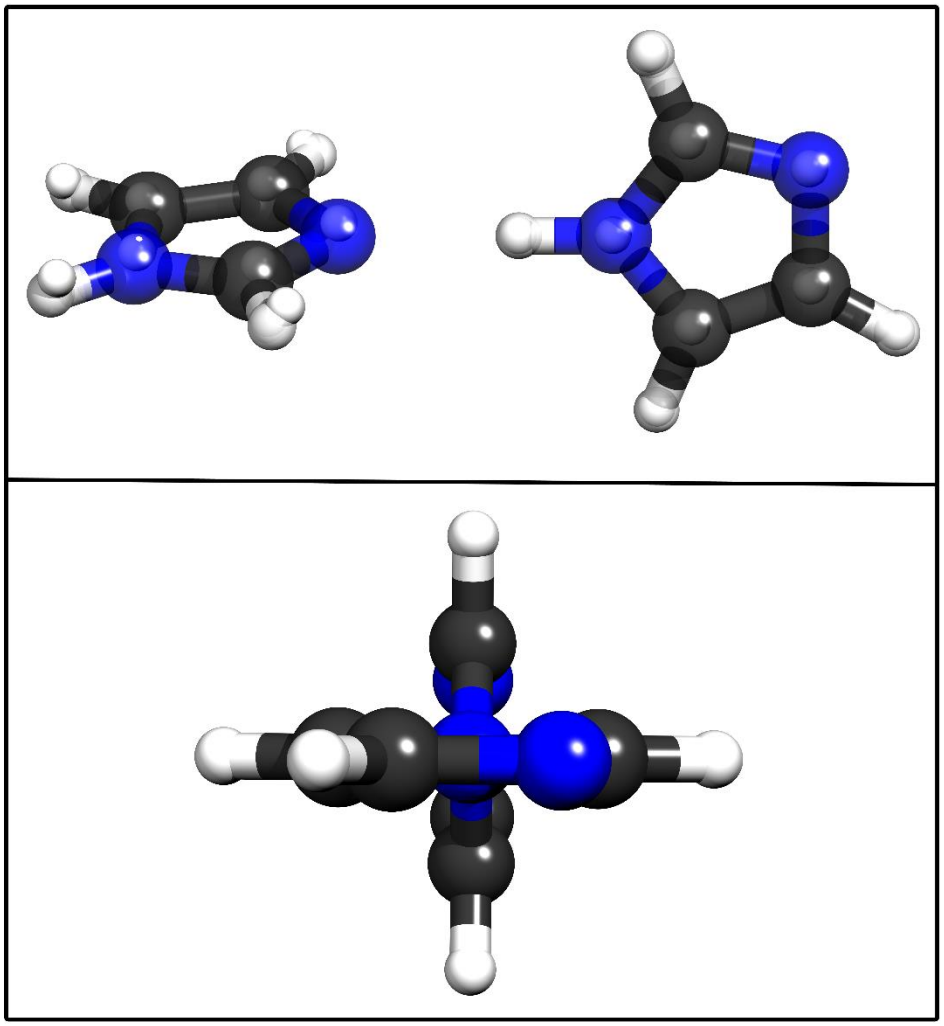

Figure 2

(Top panel) A front view of the hydrogen-bonded geometry of the imidazole dimer calculated to be the lowest energy conformer. The geometry determined from the experimentally-measured rotational constants (atoms represented by smaller spheres) is overlaid with the results of the CCSD(T)(F12*)/cc-pVDZ-F12 calculation (larger spheres). The small differences between experimental and theoretical results are evident in the coordinates of atoms within the imidazole ring

acting as H-bond acceptor. (Bottom panel) A side view of the geometry shown in the top panel illustrating the "twist" angle ($\gamma = 87.9(4)°$) in the r_0 geometry.

Figure 3

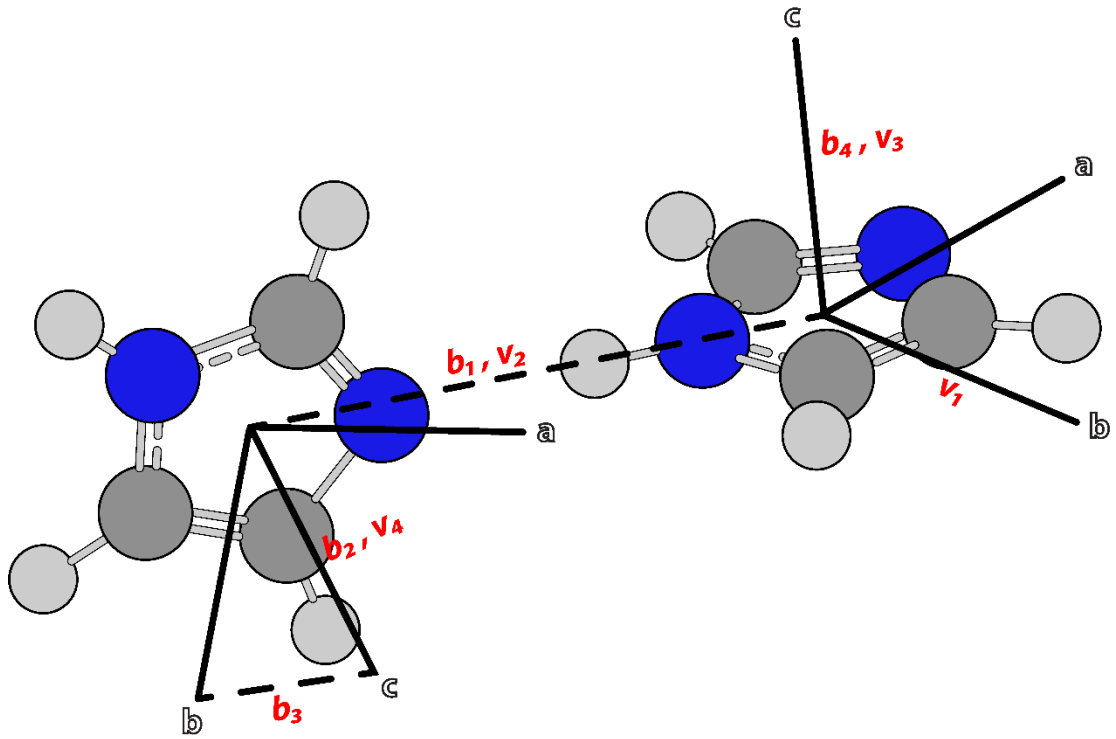

Figure 3

Angles in the model geometry of the complex are related to the displayed vectors as described in the text where $|v_n|$ are defined as magnitude vectors and b_n are normalized vectors.

References

[1] a) C. Helene, *Nature* **1998**, *391*, 436; b) S. White, J. W. Szewczyk, J. M. Turner, E. E. Baird, P. B. Dervan, *Nature* **1998**, *391*, 468; c) S. Karthikeyan, S. Nagase, *J. Phys. Chem. A* **2012**, *116*, 1694; d) Z.-F. Tao, T. Fujiwara, I. Saito, H. Sugiyama, *J. Am. Chem. Soc.* **1999**, *121*, 4961; e) S. Carles, F. Lecomte, J. P. Schermann, C. Desfrançois, *J. Phys. Chem. A* **2000**, *104*, 10662.

[2] a) M. Y. Choi, R. E. Miller, *J. Phys. Chem. A* **2006**, *110*, 9344-9351; b) M. Y. Choi, R. E. Miller, *Chem. Phys. Lett.* **2009**, *477*, 276.

[3] a) R. E. Miller, M. Y. Choi, J.-H. Lee, S. M. Hong, H. J. Jung, Y. Kim, A. Min, S. Lee, S. J. Lee, A. Ahn, *Bull. Korean Chem. Soc.* **2011**, *32*, 1407; b) R. E. Miller, M. Y. Choi, A. Min, Y. Kim, A. Ahn, S. J. Lee, S. Lee, *Bull. Korean Chem. Soc.* **2011**, *32*, 885.

[4] a) R. Ziessel, G. Ulrich, A. Harriman, *New J. Chem.* **2007**, *31*, 496; b) S. Kolemen, O. A. Bozdemir, Y. Cakmak, G. Barin, S. Erten-Ela, M. Marszalek, J.-H. Yum, S. M. Zakeeruddin, M. K. Nazeeruddin, M. Gratzel, E. U. Akkaya, *Chem. Sci.* **2011**, *2*, 949; c) G. Ulrich, R. Ziessel, A. Harriman, *Angew. Chem. Int. Ed.* **2008**, *47*, 1184; *Angew. Chem.* **2008**, *120*, 1202.

[5] a) M. N. R. Ashfold, B. Cronin, A. L. Devine, R. N. Dixon, M. G. D. Nix, *Science* **2006**, *312*, 1637; b) C. Ma, C. C.-W. Cheng, C. T.-L. Chan, R. C.-T. Chan, W.-M. Kwok, *Phys. Chem. Chem. Phys.* **2015**, *17*, 19045; c) V. Poterya, V. Profant, M. Fárník, L. Šištík, P. Slavíček, U. Buck, *J. Phys. Chem. A* **2009**, *113*, 14583; d) M. Sapunar, A. Ponzi, S. Chaiwongwattana, M. Malis, A. Prlj, P. Decleva, N. Doslic, *Phys. Chem. Chem. Phys.* **2015**, *17*, 19012.

[6] D. P. Zaleski, S. L. Stephens, N. R. Walker, *Phys. Chem. Chem. Phys.* **2014**, *16*, 25221.

[7] D. Christen, H. Griffiths John, J. Sheridan, *Z. Naturfosch., A: Phys. Sci.* **1981**, *36*, 1378.

[8] M. Kessler, H. Ring, R. Trambarulo, W. Gordy, *Phys. Rev.* **1950**, *79*, 54.

[9] V. W. Laurie, *J. Chem. Phys.* **1959**, *31*, 1500.

[10] W. S. Wilcox, J. H. Goldstein, J. W. Simmons, *J. Chem. Phys.* **1954**, *22*, 516.

[11] A. A. Westenberg, E. B. Wilson, *J. Am. Chem. Soc.* **1950**, *72*, 199.

[12] J. N. Macdonald, J. K. Tyler, *J. Chem. Soc., Chem. Commun.* **1972**, 995.

[13] A. J. Alexander, H. W. Kroto, D. R. M. Walton, *J. Mol. Spectrosc.* **1976**, *62*, 175.

[14] J. Cernicharo, R. Bachiller, G. Duvert, *Astron. Astophys.* **1986**, *160*, 181.

[15] A. Moïses, D. Boucher, J. Burie, J. Demaison, A. Dubrulle, *J. Mol. Spectrosc.* **1982**, *92*, 497.

[16] a) C. Karunatilaka, A. J. Shirar, G. L. Storck, K. M. Hotopp, E. B. Biddle, R. Crawley, B. C. Dian, *J. Phys. Chem. Lett.* **2010**, *1*, 1547; b) K. Prozument, R. G. Shaver, M. A. Ciuba, J. S. Muenter, G. B. Park, J. F. Stanton, H. Guo, B. M. Wong, D. S. Perry, R. W. Field, *Faraday Discuss.* **2013**, *163*, 33; c) K. Prozument, G. Barratt Park, R. G. Shaver, A. K. Vasiliou, J. M. Oldham, D. E. David, J. S. Muenter, J. F. Stanton, A. G. Suits, G. Barney Ellison, R. W. Field, *Phys. Chem. Chem. Phys.* **2014**, *16*, 15739.

[17] A. L. Devine, B. Cronin, M. G. D. Nix, M. N. R. Ashfold, *J. Chem. Phys.* **2006**, *125*, 184302.

[18] a) C. Hättig, W. Klopper, A. Köhn, D. P. Tew, *Chem. Rev.* **2012**, *112*, 4; b) C. Hättig, D. P. Tew, A. Köhn, *J. Chem. Phys.* **2010**, *132*, 231102.

[19] A. J. Fillery-Travis, A. C. Legon. L. C. Willoughby, *Chem. Phys. Lett.* **1983**, 102, 126.

[20] G. Winnewisser, *J. Chem. Phys.* **1972**, 54, 1803.

[21] G. Winnewisser, *J. Chem. Phys.* **1972**, 56, 2944.

[22] C. M. Western *PGOPHER, a Program for Simulating Rotational, Vibrational and Electronic Structure*; University of Bristol, http://pgopher.chm.bris.ac.uk

[23] J. K. G. Watson, *Vibrational Spectra and Structure*, Elsevier, Amsterdam, **1977**.
[24] Z. Kisiel, *J. Mol. Spectrosc.* **2003**, *218*, 58.
[25] a) E. J. Cocinero, A. Lesarri, P. Ecija, F. J. Basterretxea, J. Grabow, J. A. Fernandez, F. Castano, *Angew. Chem. Int. Ed.* **2012**, *51*, 3119; *Angew. Chem.* **2012**, *124*, 3173; b) B. M. Giuliano, L. Bizzocchi, S. Cooke, D. Banser, M. Hess, J. Fritzsche, J. Grabow, Phys. Chem. Chem. Phys. **2008**, *10*, 2078; c) B. A. Timp, J. L. Doran, S. Iyer, J. Grabow, K. R. Leopold, *J. Mol. Spectrosc.* **2012**, *271*, 20.